



Nonperturbative Renormalization of the Quasi-PDF and Its Matching

Yong Zhao

Massachusetts Institute of Technology

04/17/2019

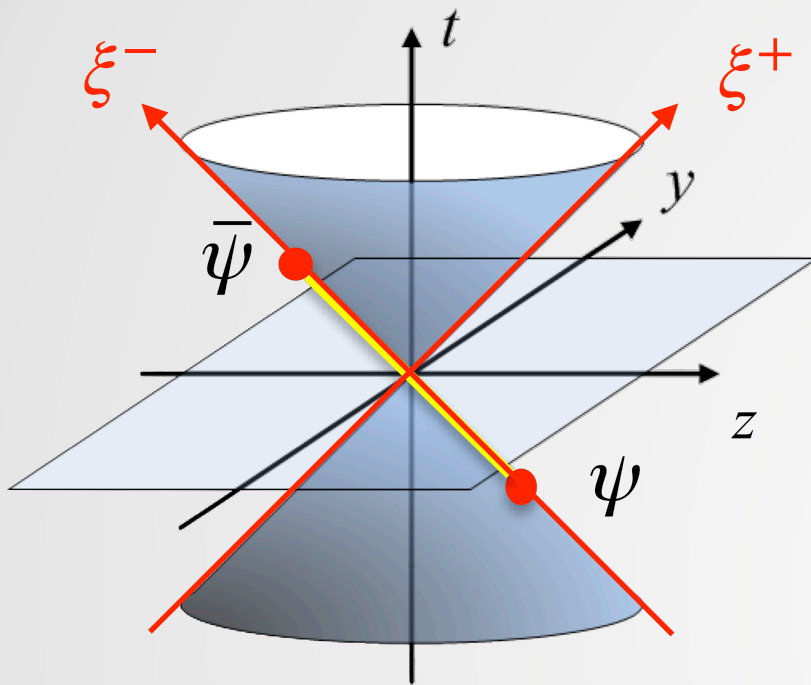
CFNS Workshop on Lattice Parton Distribution Functions
Brookhaven National Laboratory, NY, 17-19, April 2019

Outline

- **Renormalization**
 - Renormalizability of the quasi-PDF
 - Nonperturbative renormalization on lattice
- **Perturbative matching**
 - One-step matching
 - Two-step matching: “Ratio” and “Modified-MSbar” schemes
 - Comparison

Large-momentum effective theory (LaMET)

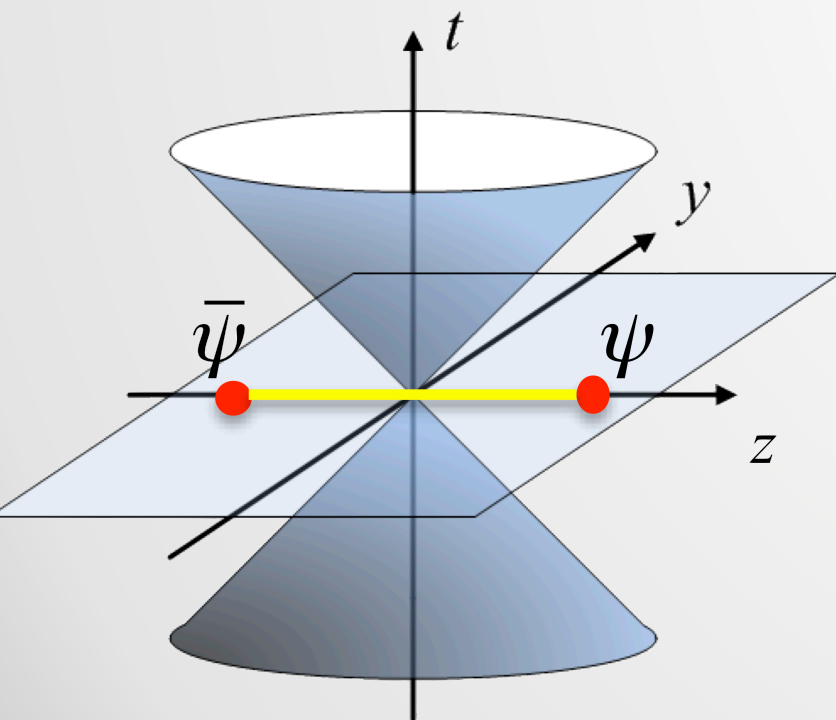
• Ji, PRL110 (2013), SCPMA57 (2014).



Light-cone PDF:

$$q(x, \mu) = \int \frac{d\xi^-}{2\pi} e^{-i\xi^-(xP^+)} \langle P | \bar{\psi}(\xi^-) \frac{\gamma^+}{2} W[\xi^-, 0] \psi(0) | P \rangle$$

$$\xi^\pm = \frac{t \mp z}{\sqrt{2}}$$



Quasi-PDF:

$$\tilde{q}(x, P^z, \mu) = \int \frac{dz}{2\pi} e^{iz(xP^z)} \langle P | \bar{\psi}(z) \frac{\Gamma}{2} W[z, 0] \psi(0) | P \rangle$$

$$\Gamma = \gamma^z \text{ or } \gamma^t$$


Systematic procedure of calculating the PDFs

$$\tilde{q}(x, P^z, \mu) = \int \frac{dy}{|y|} C\left(\frac{x}{y}, \frac{\mu}{yP^z}\right) q(y, \mu) + O\left(\frac{M^2}{P_z^2}, \frac{\Lambda_{\text{QCD}}^2}{x^2 P_z^2}\right)$$

- X. Xiong, X. Ji, J.-H. Zhang and Y.Z., PRD90 (2014);
- Y.-Q. Ma and J. Qiu, PRD98 (2018), PRL 120 (2018);
- T. Izubuchi, X. Ji, L. Jin, I. Stewart, and Y.Z., PRD98 (2018).


Systematic procedure of calculating the PDFs

1. Simulation of the quasi PDF in lattice QCD


$$\tilde{q}(x, P^z, \mu) = \int \frac{dy}{|y|} C\left(\frac{x}{y}, \frac{\mu}{yP^z}\right) q(y, \mu) + O\left(\frac{M^2}{P_z^2}, \frac{\Lambda_{\text{QCD}}^2}{x^2 P_z^2}\right)$$

- X. Xiong, X. Ji, J.-H. Zhang and Y.Z., PRD90 (2014);
- Y.-Q. Ma and J. Qiu, PRD98 (2018), PRL 120 (2018);
- T. Izubuchi, X. Ji, L. Jin, I. Stewart, and Y.Z., PRD98 (2018).

Systematic procedure of calculating the PDFs

$$\tilde{q}(x, P^z, \mu) = \int \frac{dy}{|y|} C\left(\frac{x}{y}, \frac{\mu}{yP^z}\right) q(y, \mu) + O\left(\frac{M^2}{P_z^2}, \frac{\Lambda_{\text{QCD}}^2}{x^2 P_z^2}\right)$$


2. Renormalization of the lattice quasi PDF, and then taking the continuum limit

Nonperturbative renormalization on the lattice:

- I. Stewart and Y.Z., PRD97 (2018);
- J.-W. Chen, Y.Z. et al., LP3 Collaboration, PRD97 (2018).
- Constantinou and Panagopoulos, PRD96 (2017);
- C. Alexandrou et al., ETM Collaboration, NPB923 (2017).

Systematic procedure of calculating the PDFs

- O Nachtmann, NPB63 (1973);
- J.W. Chen et al. (LP3), NPB911 (2016).

3. Subtraction of power corrections

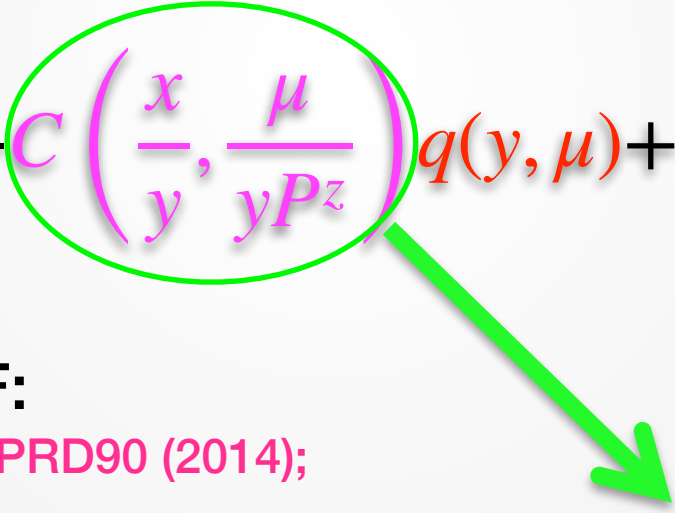
$$\tilde{q}(x, P_z, \mu) = \int \frac{dy}{|y|} C\left(\frac{x}{y}, \frac{\mu}{yP_z}\right) q(y, \mu) + O\left(\frac{M^2}{P_z^2}, \frac{\Lambda_{\text{QCD}}^2}{x^2 P_z^2}\right)$$

$q(x) \cdot O\left(\frac{\Lambda_{\text{QCD}}^2}{x^2(1-x)P_z^2}\right)$

Renormalon contribution to the power correction:

Braun, Vladimirov, and Zhang, PRD99 (2019).

Systematic procedure of calculating the PDFs

$$\tilde{q}(x, P^z, \mu) = \int \frac{dy}{|y|} C\left(\frac{x}{y}, \frac{\mu}{yP^z}\right) q(y, \mu) + O\left(\frac{M^2}{P_z^2}, \frac{\Lambda_{\text{QCD}}^2}{x^2 P_z^2}\right)$$


- Matching for the quasi-PDF:

- X. Xiong, X. Ji, J.-H. Zhang and Y.Z., PRD90 (2014);
- I. Stewart and Y.Z., PRD97 (2018);
- Y.-S. Liu, Y.Z. et al. (LP3), arXiv:1807.06566;
- T. Izubuchi, X. Ji, L. Jin, I. Stewart, and Y.Z., PRD98 (2018);
- Y.-S. Liu, Y.Z. et al., arXiv:1810.10879;
- Y.Z., Int.J.Mod.Phys. A33 (2019);
- C. Alexandrou et al. (ETMC), arXiv:1902.00587.

4. Matching to the PDF.

- The gluon case:

- W. Wang, S. Zhao, and R. Zhu, EPJC 78 (2018);
- W. Wang and S. Zhao, JHEP 05 (2018);
- W. Wang, J.-H. Zhang, S. Zhao, and R. Zhu, arXiv: 1904.00978.

Systematic procedure of calculating the PDFs

5. Extract $q(y)$

$$\tilde{q}(x, P^z, \mu) = \int \frac{dy}{|y|} C\left(\frac{x}{y}, \frac{\mu}{yP^z}\right) q(y, \mu) + O\left(\frac{M^2}{P_z^2}, \frac{\Lambda_{\text{QCD}}^2}{x^2 P_z^2}\right)$$

4. Matching to the PDF.

- Matching for the quasi-PDF:

- X. Xiong, X. Ji, J.-H. Zhang and Y.Z., PRD90 (2014);
- I. Stewart and Y.Z., PRD97 (2018);
- Y.-S. Liu, Y.Z. et al. (LP3), arXiv:1807.06566;
- T. Izubuchi, X. Ji, L. Jin, I. Stewart, and Y.Z., PRD98 (2018);
- Y.-S. Liu, Y.Z. et al., arXiv:1810.10879;
- Y.Z., Int.J.Mod.Phys. A33 (2019);
- C. Alexandrou et al. (ETMC), arXiv:1902.00587.

- The gluon case:

- W. Wang, S. Zhao, and R. Zhu, EPJC 78 (2018);
- W. Wang and S. Zhao, JHEP 05 (2018);
- W. Wang, J.-H. Zhang, S. Zhao, and R. Zhu, arXiv: 1904.00978.

Renormalization of the Wilson-line operator

Multiplicative renormalizability in coordinate space:

$$\tilde{O}(z, \mu) = Z_{j_1}^{-1} Z_{j_2}^{-1} e^{-\delta m |z|} \tilde{O}(z, \epsilon)$$

- δm renormalizes linear divergence in Wilson line self energy (under a gauge invariant UV regularization);
- Z_j renormalizes logarithmic divergences.

- X. Ji, J.-H. Zhang, and Y.Z., PRL120 (2018);
- J. Green et al., PRL121 (2018);
- T. Ishikawa, Y.-Q. Ma, J. Qiu, S. Yoshida, PRD96 (2017).

Gluon case:

- Zhang et al., PRL 122 (2019);
- Li et al., PRL122 (2019);

Renormalization on lattice

- **Lattice perturbation theory;**
 - Xiong, Luu, and Meißner, arXiv:1705.00246;
 - Ishikawa, Ma, Qiu and Yoshida, arXiv:1609.02018;
 - Constantinou and Panagopoulos, PRD96 (2017);
- **Static quark-antiquark potential;**
 - B. Musch et al., PRD 83 (2011);
 - Ishikawa, Ma, Qiu and Yoshida, arXiv:1609.02018;
 - J.-H. Zhang et al. (LP3), PRD 95 (2017).
- **Smeared quasi-PDF in the gradient flow method;**
 - C. Monahan and K. Orginos, JHEP 1703 (2017);
 - C. Monahan, PRD 97 (2018)
- **Regularization-independent momentum subtraction (RI/MOM) scheme;**
 - I. Stewart and Y.Z., PRD97 (2018);
 - J.-W. Chen, Y.Z. et al., LP3 Collaboration, PRD97 (2018).
 - Constantinou and Panagopoulos, PRD96 (2017);
 - C. Alexandrou et al., ETM Collaboration, NPB923 (2017).
- **Reduced Ioffe-time distribution.**
 - can be regarded as a nonperturbative renormalization at short distances.

A. Radyushkin, PRD96 (2017); K. Orginos et al., PRD96 (2017).

RI/MOM Scheme

Green's function:

$$G(z, p) = \sum_x \left\langle \gamma_5 S^\dagger(p, z+x) \gamma_5 U(z+x, x) \frac{\Gamma}{2} S(p, x) \right\rangle$$

Amputated Green's function
(or vertex function):

$$\Lambda(z, p) = \left(\gamma_5 [S^{-1}(p)]^\dagger \right) G(z, p) S^{-1}(p)$$

Momentum subtraction
condition:

$$Z_{\mathcal{O}}^{-1}(z, p_z^R, \mu_R) G(z, p) \Big|_{p_\mu = p_\mu^R} = G^{\text{tree}}(z, p) = e^{ip \cdot z} \Gamma$$

- RI/MOM:**
- I. Stewart and Y.Z., PRD97 (2018);
 - J.-W. Chen, Y.Z. et al., LP3 Collaboration, PRD97 (2018).

$$Z_{\mathcal{O}}^{-1}(z, p_z^R, \mu_R) Z_q(\mu_R) G(z, p) \Big|_{p_\mu = p_\mu^R} = G^{\text{tree}}(z, p), \quad Z_q(\mu_R) = \frac{1}{12} \text{Tr} [S^{-1}(p) S^{\text{tree}}(p)] \Big|_{p^2 = \mu_R^2}$$

- RI/MOM':**
- Constantinou and Panagopoulos, PRD96 (2017);
 - C. Alexandrou et al., ETM Collaboration, NPB923 (2017).

In continuum theory, there is no difference at one-loop order in the **Landau gauge**, because the quark wavefunction renormalization is zero.

Choice of projection operator

- Parametrization of amputated Green's functions:

$$\Lambda_{\gamma^t}(z, p) = \tilde{F}_t \gamma^t + \tilde{F}_z \frac{p^t \gamma^z}{p^z} + \tilde{F}_{\not{p}} \frac{p^t \not{p}}{p^2}$$

$$\Lambda_{\gamma^z}(z, p) = \tilde{F}_z \gamma^z + \tilde{F}_{\not{p}} \frac{p^z \not{p}}{p^2}$$

- Red terms which are proportional to the tree-level Green's functions include all the UV divergences;
- Choice of projection must include the red terms.

Minimal projection: $\text{Tr} \left[\Lambda_{\gamma^t}(z, p) P_{mp} \right] = \tilde{F}_t$ • Y.-S. Liu, Y.Z. et al. (LP3), arXiv:1807.06566.

P-slash projection: $\text{Tr} \left[\Lambda_{\gamma^t}(z, p) \not{p} \right] / (4p^t) = \tilde{F}_t + \tilde{F}_z + \tilde{F}_{\not{p}}$

γ^t projection: $\text{Tr} \left[\Lambda_{\gamma^t}(z, p) \gamma^t \right] / 4 = \tilde{F}_t + \tilde{F}_{\not{p}} \frac{p_t^2}{p^2}$

Operator mixing on lattice

- Due to chiral symmetry breaking, the vector-like nonlocal Wilson-line operator could also mix with the scalar operator

$$\bar{\psi}(z) \mathbf{1} P \exp \left[-ig \int^z dz' A^z(z') \right] \psi(0)$$

- For $\Gamma=\gamma^z$, mixing starts at $O(a^1)$;
 - For $\Gamma=\gamma^t$, mixing starts at $O(a^0)$.
- Constantinou and Panagopoulos, PRD96 (2017);
 - J. Green et al., PRL121 (2018);
 - J. W. Chen et al. (LP3), arXiv:1710.01089.

Outline

- **Renormalization**
 - Renormalizability of the quasi-PDF
 - Nonperturbative renormalization on lattice
- **Perturbative matching**
 - One-step matching
 - Two-step matching: “Ratio” and “Modified-MSbar” schemes
 - Comparison

Regularization-independence in the renormalized quasi-PDF

- Continuum limit of the renormalized matrix element:

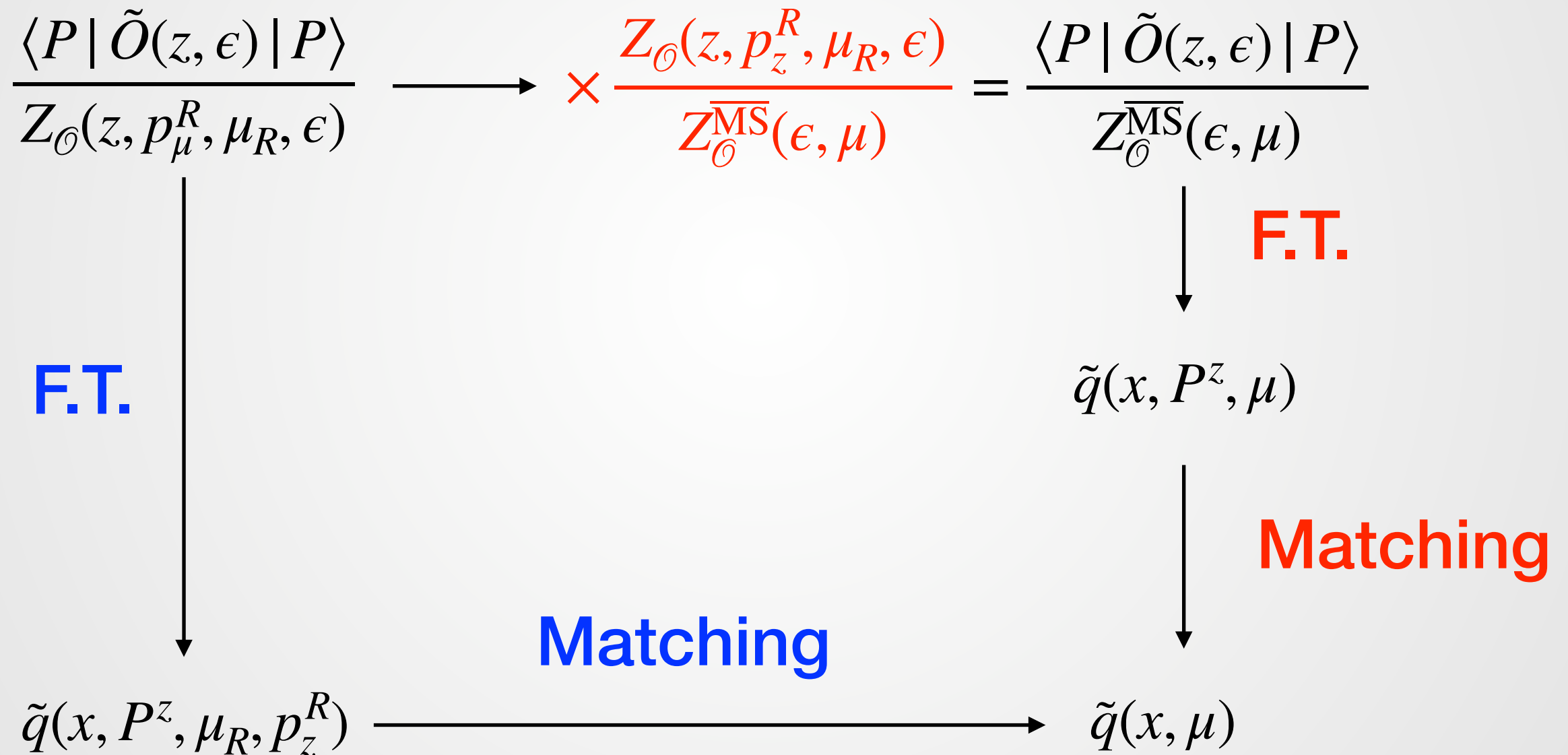
$$\lim_{a \rightarrow 0} \frac{\langle P | \tilde{O}(z, a) | P \rangle}{Z_{\mathcal{O}}(z, p_{\mu}^R, \mu_R, a)} = \frac{\langle P | \tilde{O}(z, \epsilon) | P \rangle}{Z_{\mathcal{O}}(z, p_{\mu}^R, \mu_R, \epsilon)}$$

$$D = 4 - 2\epsilon$$

- Regularization-independence allows the matching to be done in continuum perturbation theory (with dimensional regularization.)

Two matching strategies

- Constantinou and Panagopoulos, PRD96 (2017);
- C. Alexandrou et al., ETM Collaboration, NPB923 (2017).



- I. Stewart and Y.Z., PRD97 (2018);
- J.-W. Chen, Y.Z. et al., LP3 Collaboration, PRD97 (2018).

One-step matching

- Matching formula:

• I. Stewart and Y.Z., PRD97 (2018);

$$\tilde{q}(x, P^z, \mu_R, p_z^R) = \int_{-1}^1 \frac{dy}{|y|} C\left(\frac{x}{y}, r, \frac{yP^z}{\mu}, \frac{yP^z}{p_z^R}\right) q(y, \mu) + O(1/P_z^2)$$

$$r = \frac{\mu_R^2}{(p_z^R)^2}$$

- Matching kernel:

$$C\left(\xi, r, \frac{p^z}{\mu}, \frac{p^z}{p_z^R}\right) = \delta(1 - \xi) + \frac{\alpha_s C_F}{2\pi} \left[C_B\left(\xi, \frac{p^z}{\mu}\right) - \left| \frac{p^z}{p_z^R} \right| h\left(1 + \frac{p^z}{p_z^R}(\xi - 1), r\right) \right]_{+}^{(-\infty, \infty)}$$

$$\xi = \frac{x}{y}, \quad p^z = yP^z$$

$$[f(x)]_{+}^{(-\infty, \infty)} = f(x) - \delta(x - 1) \int_{-\infty}^{\infty} dy f(y)$$

- 😊 Formally satisfying vector current (or particle number conservation): $\int_{-\infty}^{\infty} d\xi C(\xi) = 1$
- 😞 Renormalization scale dependence to be cancelled in the final result, making systematics analysis more complicated.

One-step matching

For $\Gamma = \gamma^z$, Feynman Gauge

• I. Stewart and Y.Z., PRD97 (2018);

$$\left[C_B \left(\xi, \frac{p^z}{\mu} \right) \right]_+^{-\infty, \infty} = \begin{cases} \left[\frac{1 + \xi^2}{1 - \xi} \ln \frac{\xi}{\xi - 1} + 1 \right]_{\oplus} & \xi > 1 \\ \left[\frac{1 + \xi^2}{1 - \xi} \ln \frac{4(p^z)^2}{\mu^2} + \frac{1 + \xi^2}{1 - \xi} \ln [\xi(1 - \xi)] + (2 - \xi) - \frac{2\xi}{1 - \xi} \right]_+ & 0 < \xi < 1 \\ \left[\frac{1 + \xi^2}{1 - \xi} \ln \frac{\xi - 1}{\xi} - 1 \right]_{\ominus} & \xi < 0 \end{cases}$$

$$h(x, \rho) \equiv \begin{cases} \frac{1}{\sqrt{1 - \rho}} \left[\frac{1 + x^2}{1 - x} - \frac{\rho}{2(1 - x)} \right] \ln \frac{2x - 1 + \sqrt{1 - \rho}}{2x - 1 - \sqrt{1 - \rho}} - \frac{\rho}{4x(x - 1) + \rho} + 1 & x > 1 \\ \frac{1}{\sqrt{1 - \rho}} \left[\frac{1 + x^2}{1 - x} - \frac{\rho}{2(1 - x)} \right] \ln \frac{1 + \sqrt{1 - \rho}}{1 - \sqrt{1 - \rho}} - \frac{2x}{1 - x} & 0 < x < 1 \\ \frac{1}{\sqrt{1 - \rho}} \left[\frac{1 + x^2}{1 - x} - \frac{\rho}{2(1 - x)} \right] \ln \frac{2x - 1 - \sqrt{1 - \rho}}{2x - 1 + \sqrt{1 - \rho}} + \frac{\rho}{4x(x - 1) + \rho} - 1 & x < 0 \end{cases}$$

Well-behaving matching kernel

$$C\left(\xi, r, \frac{p^z}{\mu}, \frac{p^z}{p_z^R}\right) = \delta(1 - \xi) + \frac{\alpha_s C_F}{2\pi} \left[C_B\left(\xi, \frac{p^z}{\mu}\right) - \left| \frac{p^z}{p_z^R} \right| h\left(1 + \frac{p^z}{p_z^R}(\xi - 1), r\right) \right]_+^{(-\infty, \infty)}$$

Singularity at $\xi=1$ is regulated by plus function.

Asymptotic region:

$$\lim_{\xi \rightarrow \infty} C_B\left(\xi, \frac{p^z}{\mu}\right) = -\frac{3}{2|\xi|} \quad \lim_{\xi \rightarrow \infty} \left| \frac{p^z}{p_z^R} \right| h\left(1 + \frac{p^z}{p_z^R}(\xi - 1), r\right) = -\frac{3}{2|\xi|}$$

$$\lim_{\xi \rightarrow \infty} \left[C_B\left(\xi, \frac{p^z}{\mu}\right) - \left| \frac{p^z}{p_z^R} \right| h\left(1 + \frac{p^z}{p_z^R}(\xi - 1), r\right) \right] \sim \frac{1}{\xi^2}$$

$$\int_{-\infty}^{\infty} d\xi' \left[C_B\left(\xi', \frac{p^z}{\mu}\right) - \left| \frac{p^z}{p_z^R} \right| h\left(1 + \frac{p^z}{p_z^R}(\xi' - 1), r\right) \right] = \text{UV finite}$$

Two-step matching

- Scheme conversion:

- Constantinou and Panagopoulos, PRD96 (2017)

$$C(z, p_z^R, \mu_R, \mu) = \frac{Z_{\mathcal{O}}(z, p_z^R, \mu_R, \epsilon)}{Z_{\mathcal{O}}^{\overline{\text{MS}}}(\epsilon, \mu)}$$

Renormalization scale dependence to be cancelled in the first step, useful for the systematics analysis.

- Matching in the MSbar scheme:

$$\tilde{q}(x, P^z, \mu) = \int \frac{dy}{|y|} C\left(\frac{x}{y}, \frac{\mu}{yP^z}\right) q(y, \mu) + O\left(\frac{M^2}{P_z^2}, \frac{\Lambda_{\text{QCD}}^2}{x^2 P_z^2}\right)$$

- T. Izubuchi, X. Ji, L. Jin, I. Stewart, and Y.Z., PRD98 (2018)

Two-step matching

$$\begin{aligned}
 C_{V_\nu(A_\nu)} = 1 - \frac{g^2 C_f}{16 \pi^2} & \left(-7 - 4\gamma_E + \log(16) + 4F_2 + \frac{4\bar{q}_\nu^2 |z|}{\bar{q}} F_5 + (\beta - 4) \log \left(\frac{\bar{\mu}^2}{\bar{q}^2} \right) - (\beta + 2) \log(\bar{q}^2 z^2) \right. \\
 & + \beta \left[3 - 2\gamma_E + \log(4) - 2 \left(\frac{\bar{q}_\nu^2 |z|}{\bar{q}} F_4 + (\bar{q}^2 + \bar{q}_\mu^2) G_3 \right) - 2F_1 + z^2 \left(\bar{q}^2 \left(F_3 - \frac{F_1 - F_2}{2} \right) + \bar{q}_\nu^2 (F_1 - F_2 - F_3) \right) \right] \\
 & \left. + i \left\{ 4\bar{q}_\mu G_1 + \beta \bar{q}_\mu \left[\bar{q}(z|z|F_5 + 2(G_4 - 2G_5)) - 2G_1 + 2G_2 \right] \right\} \right) \quad (36)
 \end{aligned}$$

• Constantinou and Panagopoulos, PRD96 (2017)

$$\begin{aligned}
 C^{\overline{\text{MS}}} \left(\xi, \frac{\mu}{|y|P^z} \right) = \delta(1 - \xi) + \frac{\alpha_s C_F}{2\pi} & \begin{cases} \left(\frac{1 + \xi^2}{1 - \xi} \ln \frac{\xi}{\xi - 1} + 1 + \frac{3}{2\xi} \right)_{+(1)}^{[1, \infty]} - \frac{3}{2\xi} & \xi > 1 \\ \left(\frac{1 + \xi^2}{1 - \xi} \left[-\ln \frac{\mu^2}{y^2 P_z^2} + \ln(4\xi(1 - \xi)) \right] - \frac{\xi(1 + \xi)}{1 - \xi} \right)_{+(1)}^{[0, 1]} & 0 < \xi < 1 \\ \left(-\frac{1 + \xi^2}{1 - \xi} \ln \frac{-\xi}{1 - \xi} - 1 + \frac{3}{2(1 - \xi)} \right)_{+(1)}^{[-\infty, 0]} - \frac{3}{2(1 - \xi)} & \xi < 0 \end{cases} \\
 + \frac{\alpha_s C_F}{2\pi} \delta(1 - \xi) & \left(\frac{3}{2} \ln \frac{\mu^2}{4y^2 P_z^2} + \frac{5}{2} \right).
 \end{aligned}$$

• T. Izubuchi, X. Ji, L. Jin, I. Stewart, and Y.Z., PRD98 (2018)

Problems with MSbar scheme

$$\begin{aligned}
 C_{V_\nu(A_\nu)} = 1 - \frac{g^2 C_f}{16 \pi^2} & \left(-7 - 4\gamma_E + \log(16) + 4F_2 + \frac{4\bar{q}_\nu^2 |z|}{\bar{q}} F_5 + (\beta - 4) \log\left(\frac{\bar{\mu}^2}{\bar{q}^2}\right) - (\beta + 2) \log(\bar{q}^2 z^2) \right. \\
 & + \beta \left[3 - 2\gamma_E + \log(4) - 2 \left(\frac{\bar{q}_\nu^2 |z|}{\bar{q}} F_4 + (\bar{q}^2 + \bar{q}_\mu^2) G_3 \right) - 2F_1 + z^2 \left(\bar{q}^2 \left(F_3 - \frac{F_1 - F_2}{2} \right) + \bar{q}_\nu^2 (F_1 - F_2 - F_3) \right) \right] \\
 & \left. + i \left\{ 4\bar{q}_\mu G_1 + \beta \bar{q}_\mu \left[\bar{q}(z|z|F_5 + 2(G_4 - 2G_5)) - 2G_1 + 2G_2 \right] \right\} \right) \quad (36)
 \end{aligned}$$

For minimal projection

$$\lim_{z \rightarrow 0} C(z, p_z^R, \mu_R, \mu) = 1 + \frac{\alpha_s C_F}{2\pi} \left[\frac{3}{2} \ln \frac{\mu^2 z^2 e^{2\gamma_E}}{4} + \frac{5}{2} \right]$$

- Independent of p_z^R and μ_R !
- Gauge-invariant, but the constant part depends on the quark wave function renormalization scheme;
- Breaks down vector current conservation in the MSbar quasi-PDF;
- Logarithmic divergence in the local limit could be an issue when implemented numerically.

Problems with MSbar scheme

- Breaks down vector current conservation;
- This effect could cancel that from the scheme conversion so that the final PDF satisfies vector current conservation. However, such cancellation is nontrivial when implemented numerically.

$$C^{\overline{\text{MS}}} \left(\xi, \frac{\mu}{|y|P^z} \right) = \delta(1 - \xi) + \frac{\alpha_s C_F}{2\pi} \left\{ \begin{array}{ll} \left(\frac{1 + \xi^2}{1 - \xi} \ln \frac{\xi}{\xi - 1} + 1 + \frac{3}{2\xi} \right)_{+(1)}^{[1, \infty]} - \frac{3}{2\xi} & \xi > 1 \\ \left(\frac{1 + \xi^2}{1 - \xi} \left[-\ln \frac{\mu^2}{y^2 P_z^2} + \ln(4\xi(1 - \xi)) \right] - \frac{\xi(1 + \xi)}{1 - \xi} \right)_{+(1)}^{[0, 1]} & 0 < \xi < 1 \\ \left(-\frac{1 + \xi^2}{1 - \xi} \ln \frac{-\xi}{1 - \xi} - 1 + \frac{3}{2(1 - \xi)} \right)_{+(1)}^{[-\infty, 0]} - \frac{3}{2(1 - \xi)} & \xi < 0 \end{array} \right.$$

$$+ \frac{\alpha_s C_F}{2\pi} \delta(1 - \xi) \left(\frac{3}{2} \ln \frac{\mu^2}{4y^2 P_z^2} + \frac{5}{2} \right).$$

Ratio scheme

$$C^{\text{ratio}}(z, p_z^R, \mu_R, \mu) = \frac{C(z, p_z^R, \mu_R, \mu)}{1 + \frac{\alpha_s C_F}{2\pi} \left[\frac{3}{2} \ln \frac{\mu^2 z^2 e^{2\gamma_E}}{4} + \frac{5}{2} \right]} \quad \lim_{z \rightarrow 0} C(z, p_z^R, \mu_R, \mu) = 1$$

• T. Izubuchi, X. Ji, L. Jin, I. Stewart, and Y.Z., PRD98 (2018);

• Y.Z., Int.J.Mod.Phys. A33 (2019);

• A. Radyushkin, PLB781 (2018).

$$C^{\text{ratio}}\left(\xi, \frac{\mu}{|y|P^z}\right) = \delta(1 - \xi) + \frac{\alpha_s C_F}{2\pi} \begin{cases} \left(\frac{1 + \xi^2}{1 - \xi} \ln \frac{\xi}{\xi - 1} + 1 - \frac{3}{2(1 - \xi)} \right)_{+(1)}^{[1, \infty]} & \xi > 1 \\ \left(\frac{1 + \xi^2}{1 - \xi} \left[-\ln \frac{\mu^2}{y^2 P_z^2} + \ln(4\xi(1 - \xi)) - 1 \right] + 1 + \frac{3}{2(1 - \xi)} \right)_{+(1)}^{[0, 1]} & 0 < \xi < 1 \\ \left(-\frac{1 + \xi^2}{1 - \xi} \ln \frac{-\xi}{1 - \xi} - 1 + \frac{3}{2(1 - \xi)} \right)_{+(1)}^{[-\infty, 0]} & \xi < 0 \end{cases}$$

• Satisfying vector current conservation at each step;

• Well-behaving matching kernel;

$$\lim_{\xi \rightarrow \infty} C^{\text{ratio}}\left(\xi, \frac{p^z}{\mu}\right) \sim \frac{1}{\xi^2}$$

• Actually,

$$\text{F.T.} \left\{ \frac{\alpha_s C_F}{2\pi} \left[\frac{3}{2} \ln \frac{\mu^2 z^2 e^{2\gamma_E}}{4} + \frac{5}{2} \right] \right\} = C^{\overline{\text{MS}}}(\xi, \frac{\mu}{p^z}) - C^{\text{Ratio}}(\xi, \frac{\mu}{p^z})$$

Modified MSbar scheme

$$C^{\text{MMS}}(z, p_z^R, \mu_R, \mu) = \frac{C(z, p_z^R, \mu_R, \mu)}{Z_{\Gamma_{\gamma^0}}^{\text{MMS}}(z\bar{\mu})}$$

$$\lim_{z \rightarrow 0} C(z, p_z^R, \mu_R, \mu) = 1$$

$$C_{\gamma^0, \gamma^3, \gamma^3 \gamma^5}^{\text{MMS}}\left(\xi, \frac{\bar{\mu}}{p_3}\right) = \delta(1 - \xi)$$

$$Z_{\Gamma_{\gamma^0}}^{\text{MMS}}(z\bar{\mu}) = 1 - \frac{\alpha_s}{2\pi} C_F \left(\frac{3}{2} \ln\left(\frac{1}{4}\right) + \frac{5}{2} \right) + \frac{3}{2} \frac{\alpha_s}{2\pi} C_F \left(i\pi \frac{|z\bar{\mu}|}{2z\bar{\mu}} - \text{Ci}(z\bar{\mu}) + \ln(z\bar{\mu}) - \ln(|z\bar{\mu}|) - i\text{Si}(z\bar{\mu}) \right) - \frac{3}{2} \frac{\alpha_s}{2\pi} C_F e^{iz\bar{\mu}} \left(\frac{2\text{Ei}(-iz\bar{\mu}) - \ln(-iz\bar{\mu}) + \ln(iz\bar{\mu}) + i\pi \text{sgn}(z\bar{\mu})}{2} \right)$$

$$+ \frac{\alpha_s C_F}{2\pi} \begin{cases} \left(\frac{1 + \xi^2}{1 - \xi} \ln\left(\frac{\xi}{\xi - 1}\right) + 1 + \frac{3}{2\xi} \right)_{+(1)}, & \xi > 1, \\ \left(\frac{1 + \xi^2}{1 - \xi} \left[\ln\left(\frac{p_3^2}{\bar{\mu}^2}\right) + \ln(4\xi(1 - \xi)) \right] - \frac{\xi(1 + \xi)}{1 - \xi} + 2\iota(1 - \xi) \right)_{+(1)}, & 0 < \xi < 1, \\ \left(-\frac{1 + \xi^2}{1 - \xi} \ln\left(\frac{-\xi}{1 - \xi}\right) - 1 + \frac{3}{2(1 - \xi)} \right)_{+(1)}, & \xi < 0, \end{cases}$$

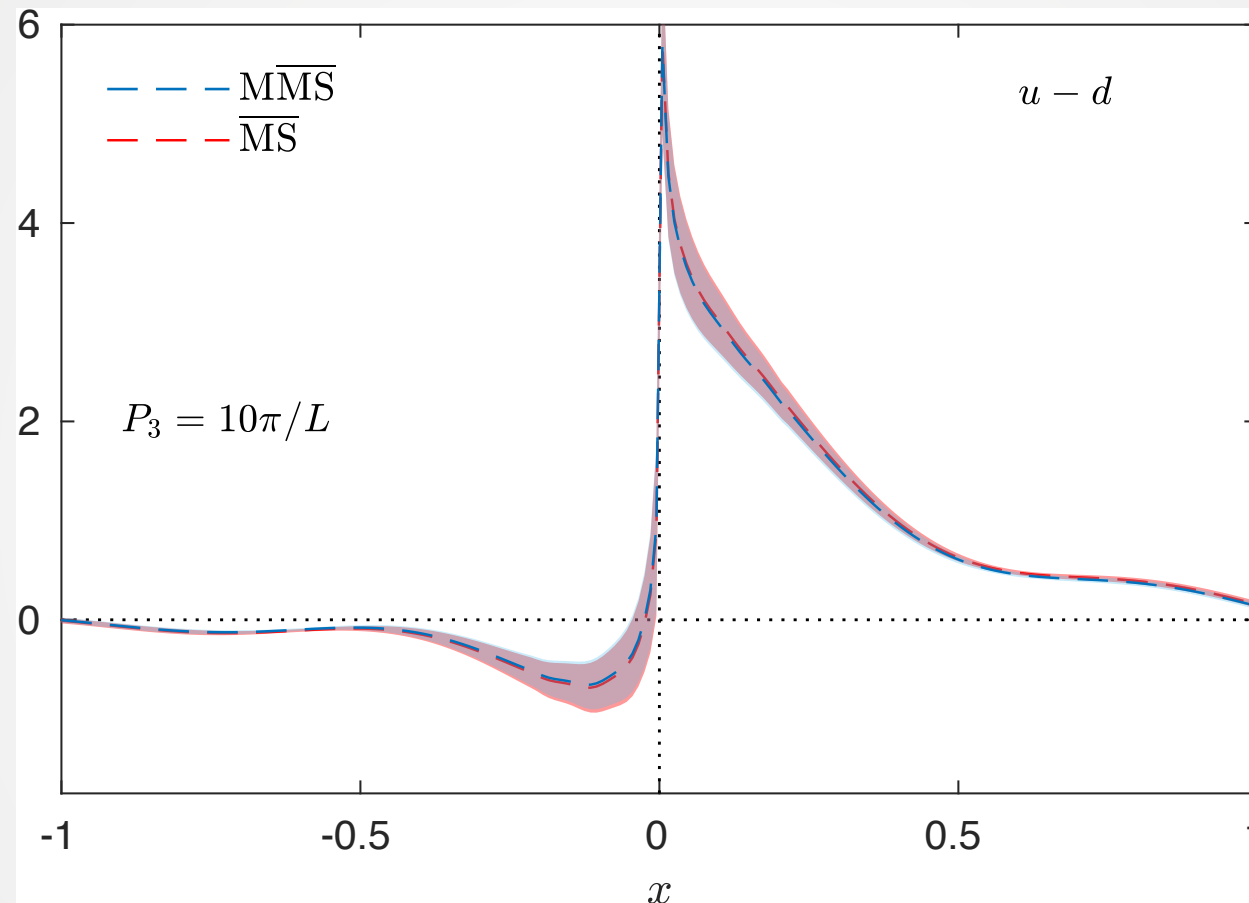
$$\text{F.T.} \left\{ Z_{\Gamma_{\gamma^0}}^{\text{MMS}}(z\mu) \right\} = C^{\text{MS}}(\xi, \frac{\mu}{p^z}) - C^{\text{MMS}}(\xi, \frac{\mu}{p^z})$$

• C. Alexandrou et al. (ETMC), arXiv:1902.00587.

Comparison among different schemes

- C. Alexandrou et al. (ETMC), [arXiv:1902.00587](#).
- There is still discrepancy among different schemes for the same lattice input data.

Comparison among different schemes

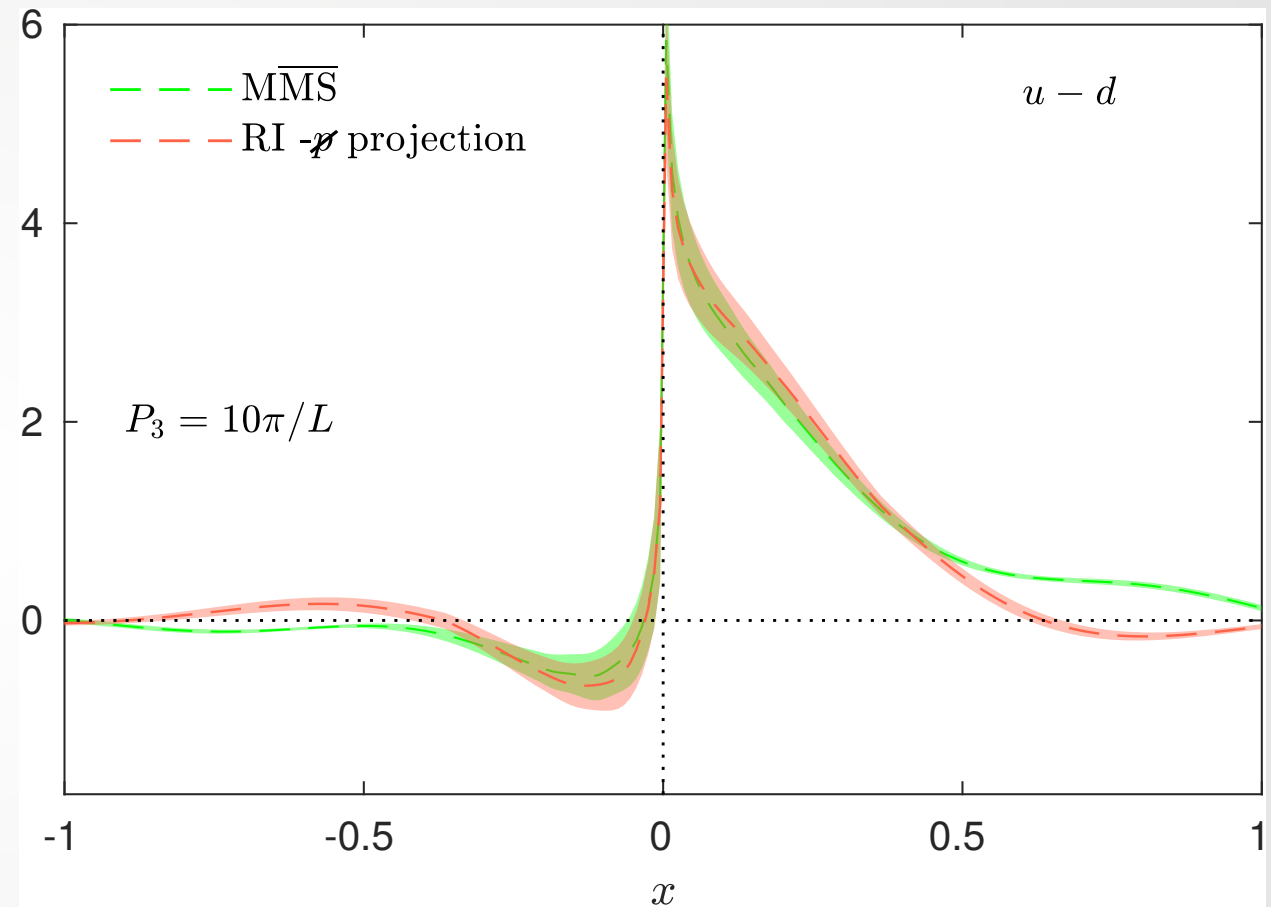
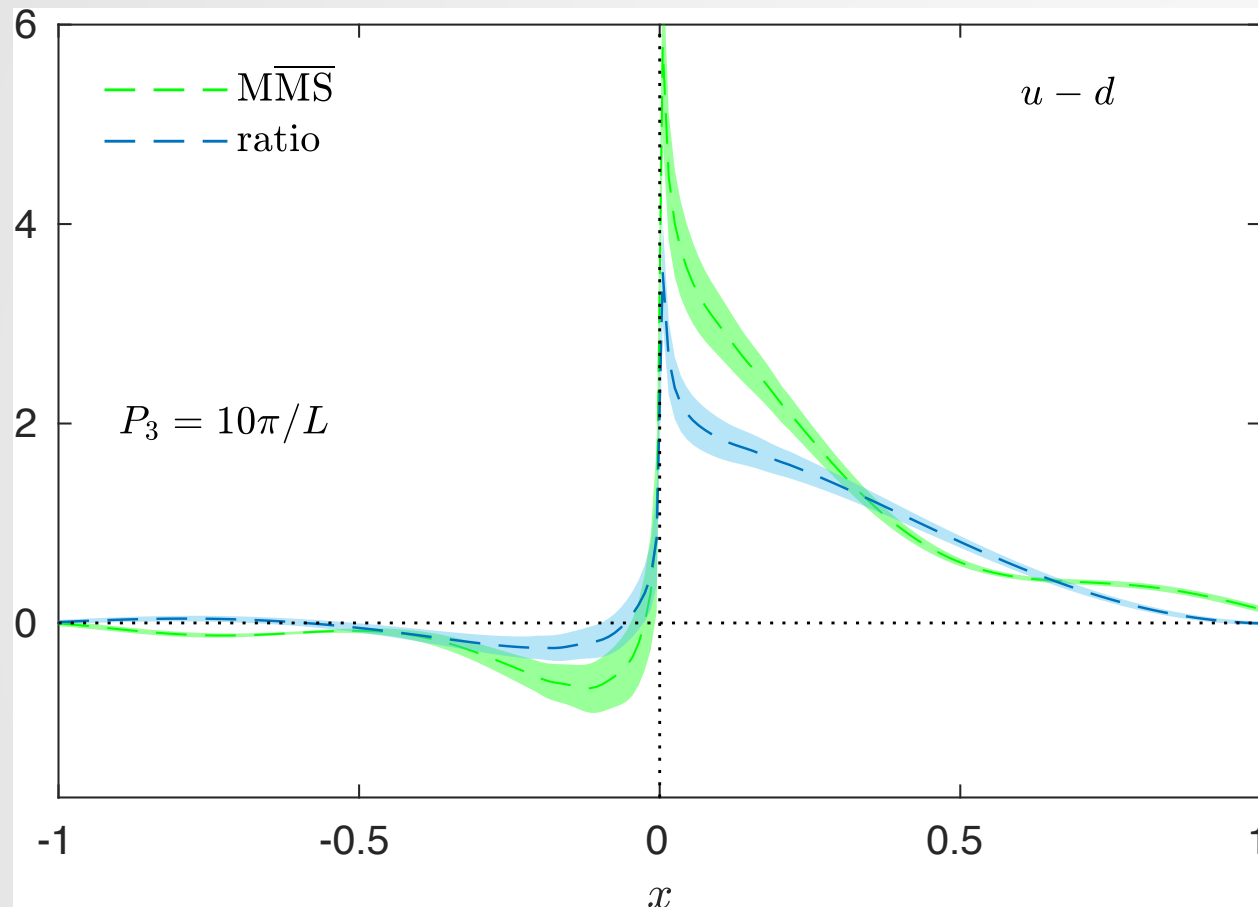


- C. Alexandrou et al. (ETMC), arXiv:1902.00587.
- There is still discrepancy among different schemes for the same lattice input data.

Comparison among different schemes

- C. Alexandrou et al. (ETMC), [arXiv:1902.00587](#).
- There is still discrepancy among different schemes for the same lattice input data.

Comparison among different schemes

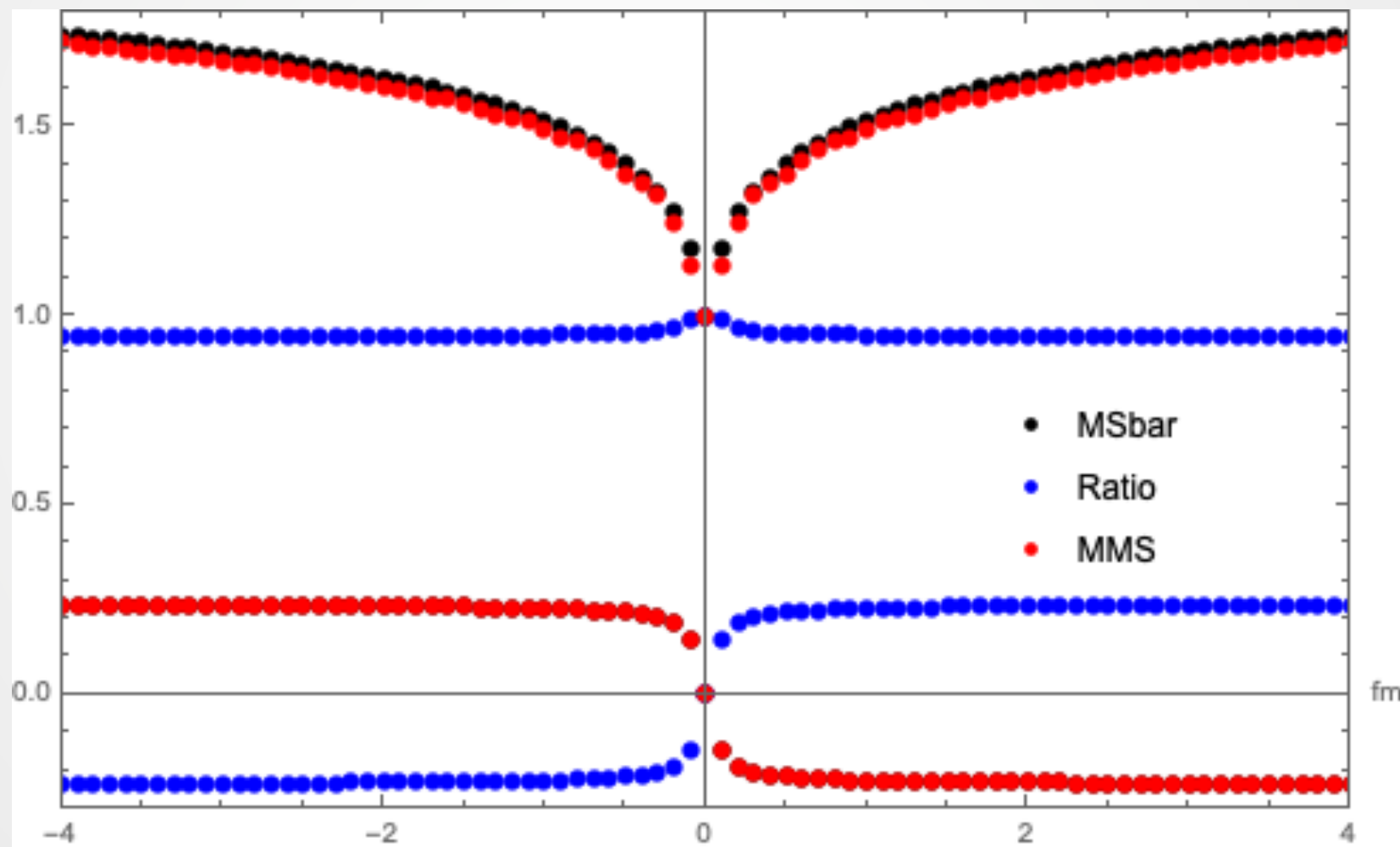


- C. Alexandrou et al. (ETMC), arXiv:1902.00587.
- There is still discrepancy among different schemes for the same lattice input data.

Re-examine the differences among various strategies and schemes

- Conversion factors:

$$P^z = 3.0 \text{ GeV}; \mu = 3.0 \text{ GeV}; p_z^R = 2.2 \text{ GeV}; \mu_R = 3.7 \text{ GeV}; \alpha_s = 0.258.$$

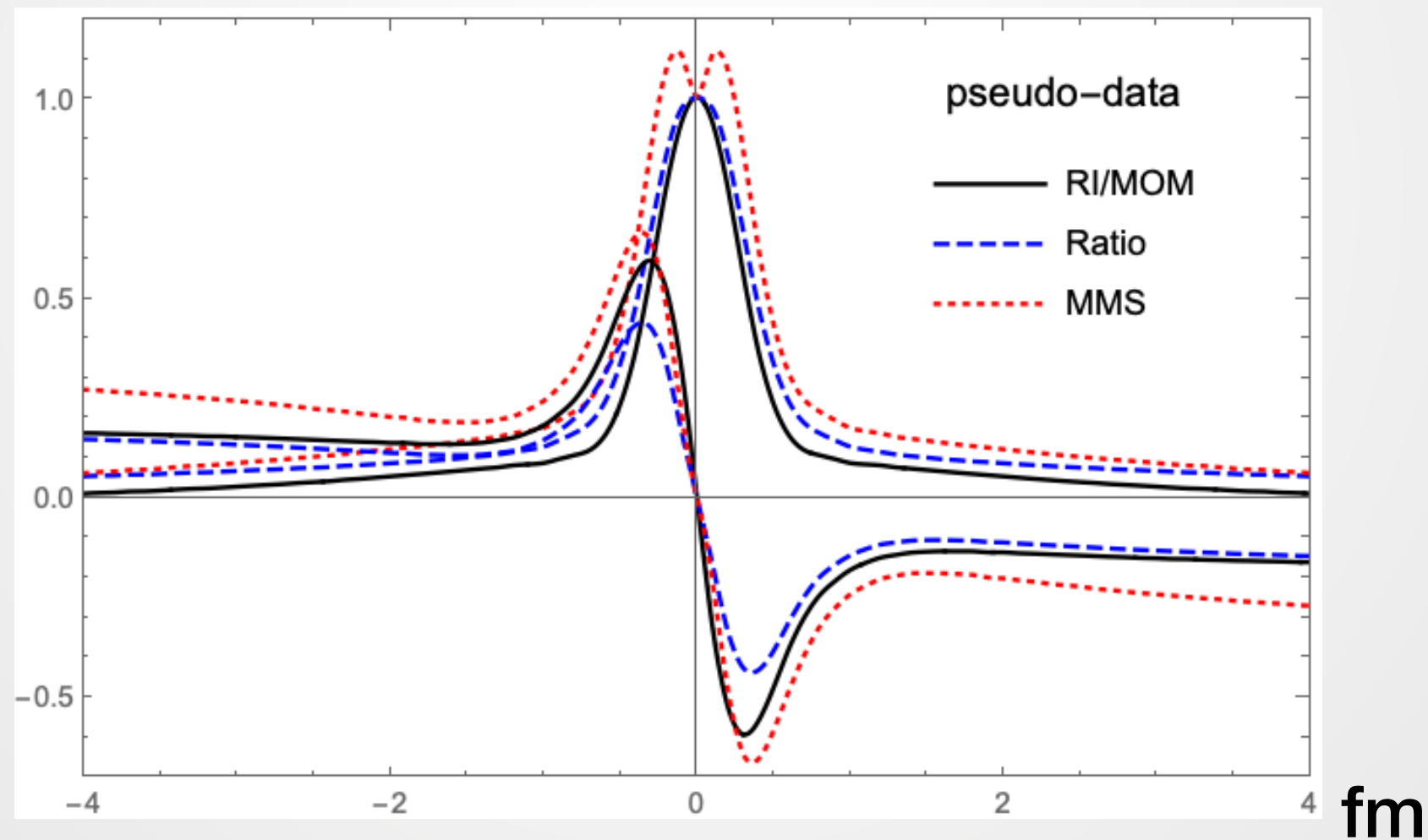


In collaboration
with Yu-Sheng Liu

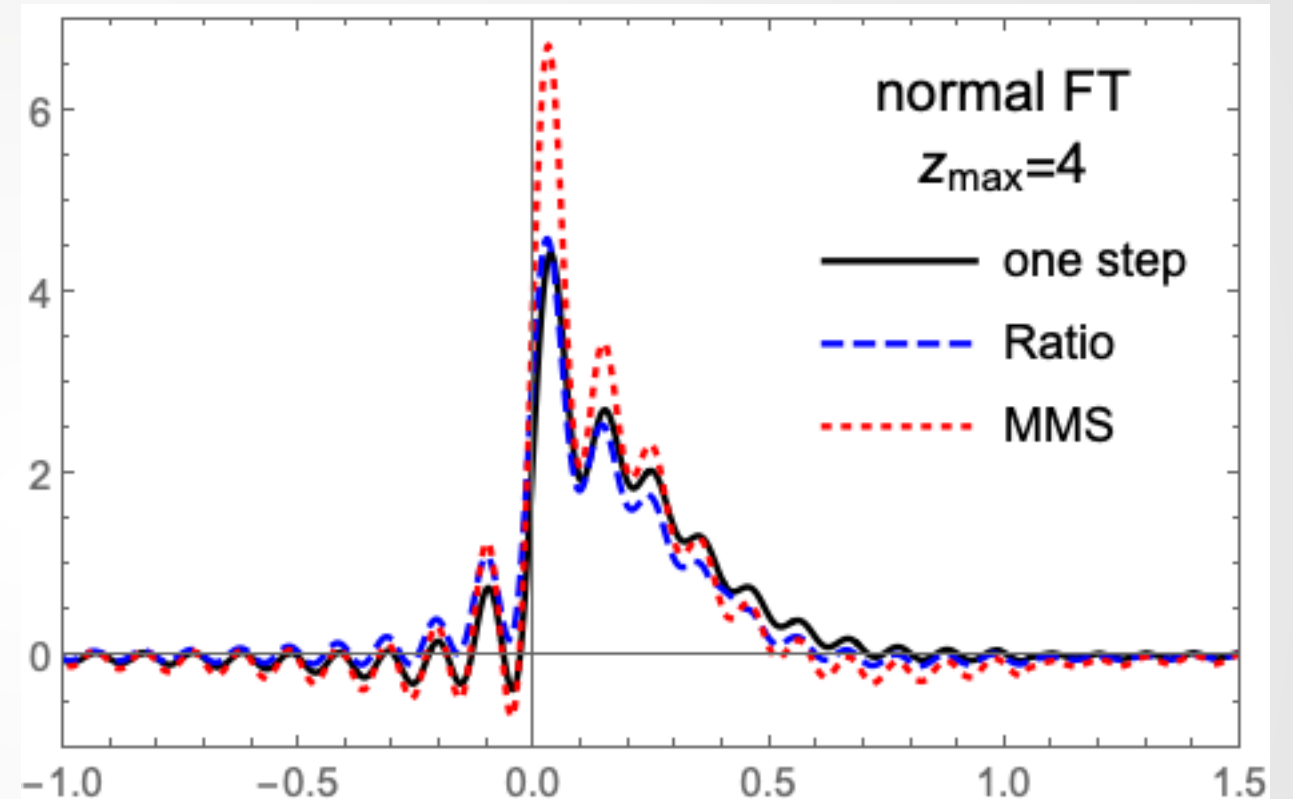
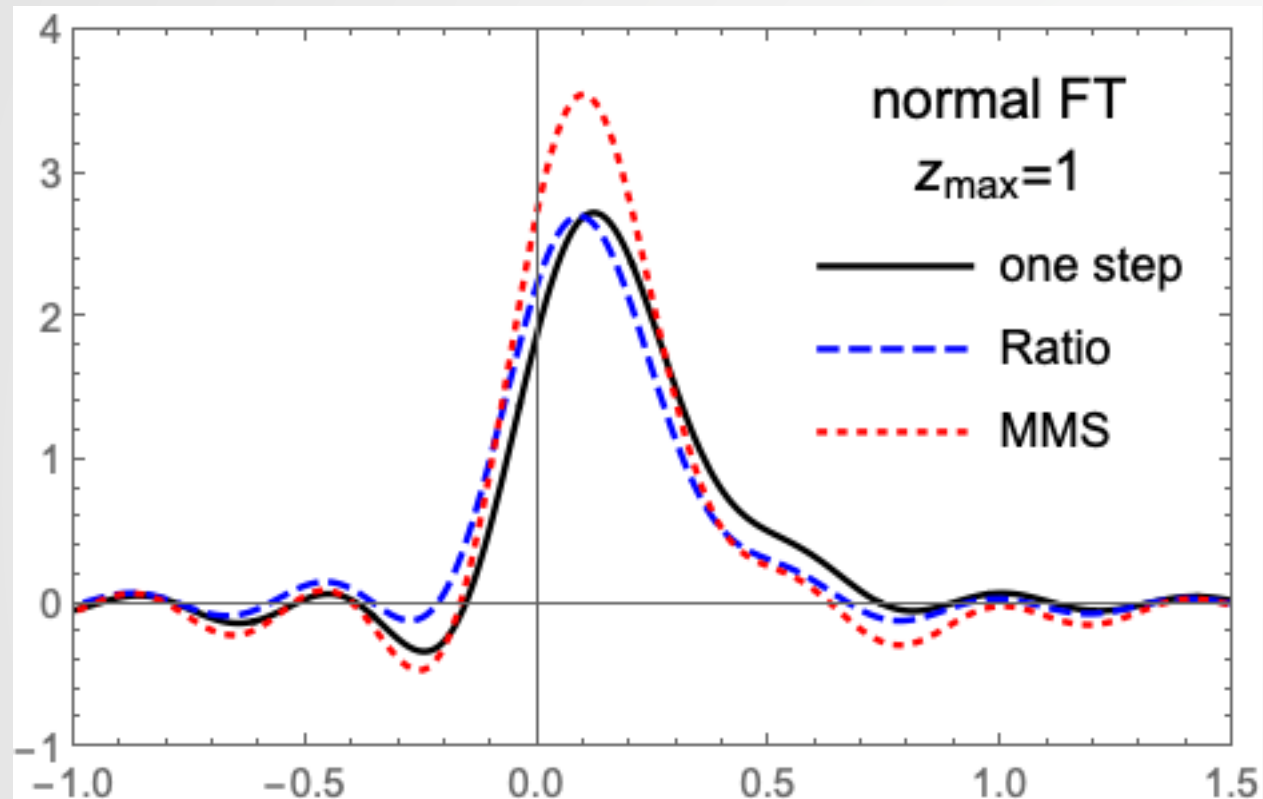
$$\int_{-z_{\max}}^{z_{\max}} \frac{d(zp^z)}{2\pi} e^{i\xi zp^z} Z_{\Gamma\gamma^0}^{\text{MMS/Ratio}}(z\mu) \neq C^{\overline{\text{MS}}}(\xi, \frac{\mu}{p^z}) - C^{\text{MMS/Ratio}}(\xi, \frac{\mu}{p^z})$$

- Conversion of pseudo data for the RI/MOM matrix element:

$$P^z = 3.0 \text{ GeV}; \mu = 3.0 \text{ GeV}; p_z^R = 2.2 \text{ GeV}; \mu_R = 3.7 \text{ GeV}; \alpha_s = 0.258.$$

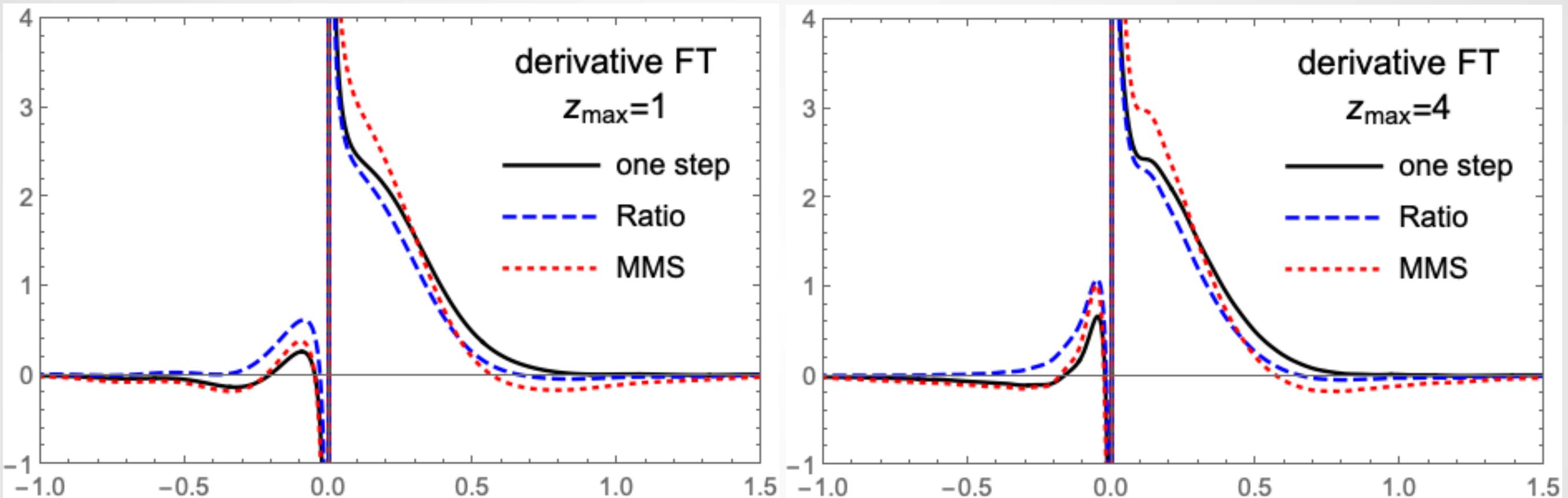


Fourier transform



“One step” standards for the pseudo RI/MOM matrix elements.

Fourier transform



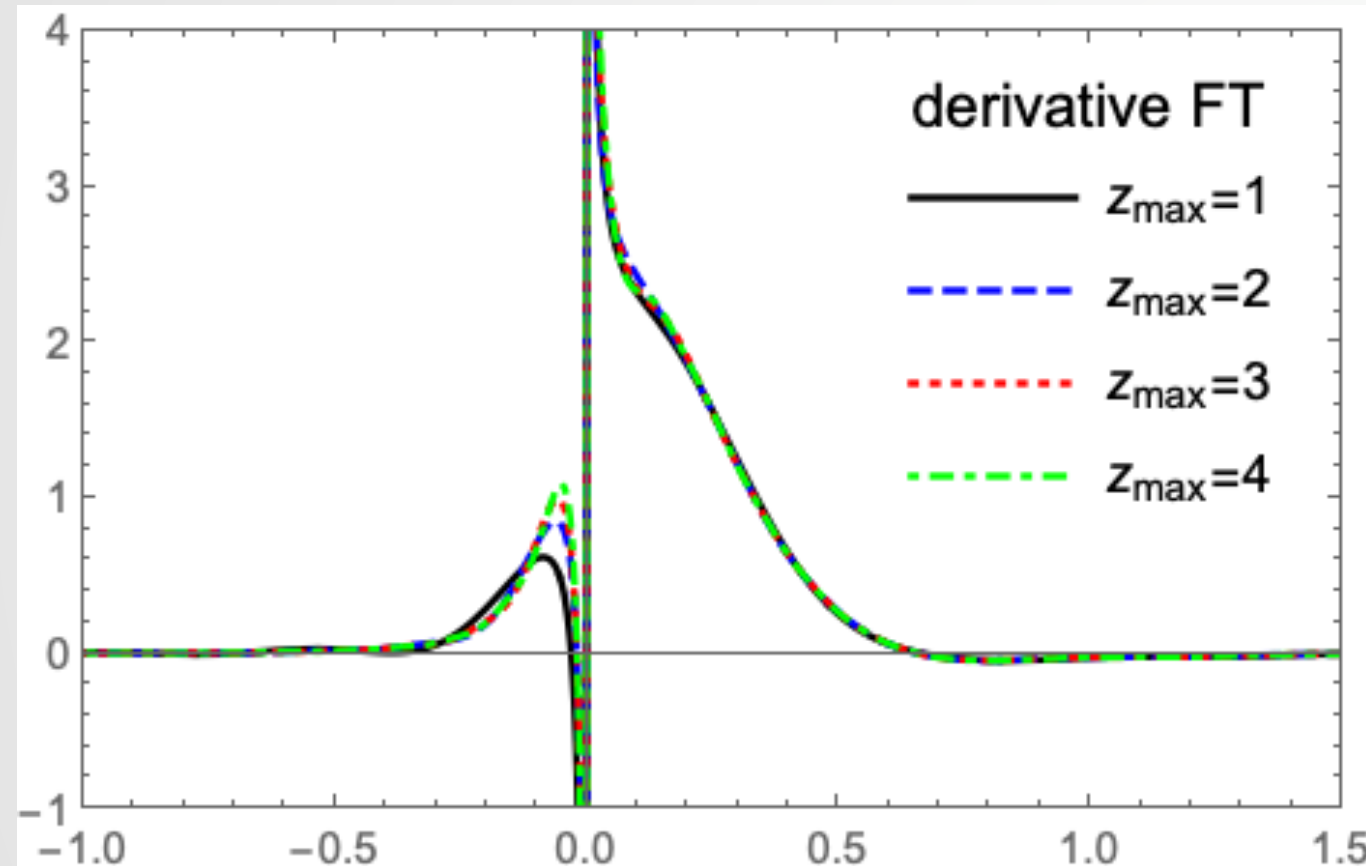
“One step” standards for the pseudo RI/MOM matrix elements.

Derivative method:

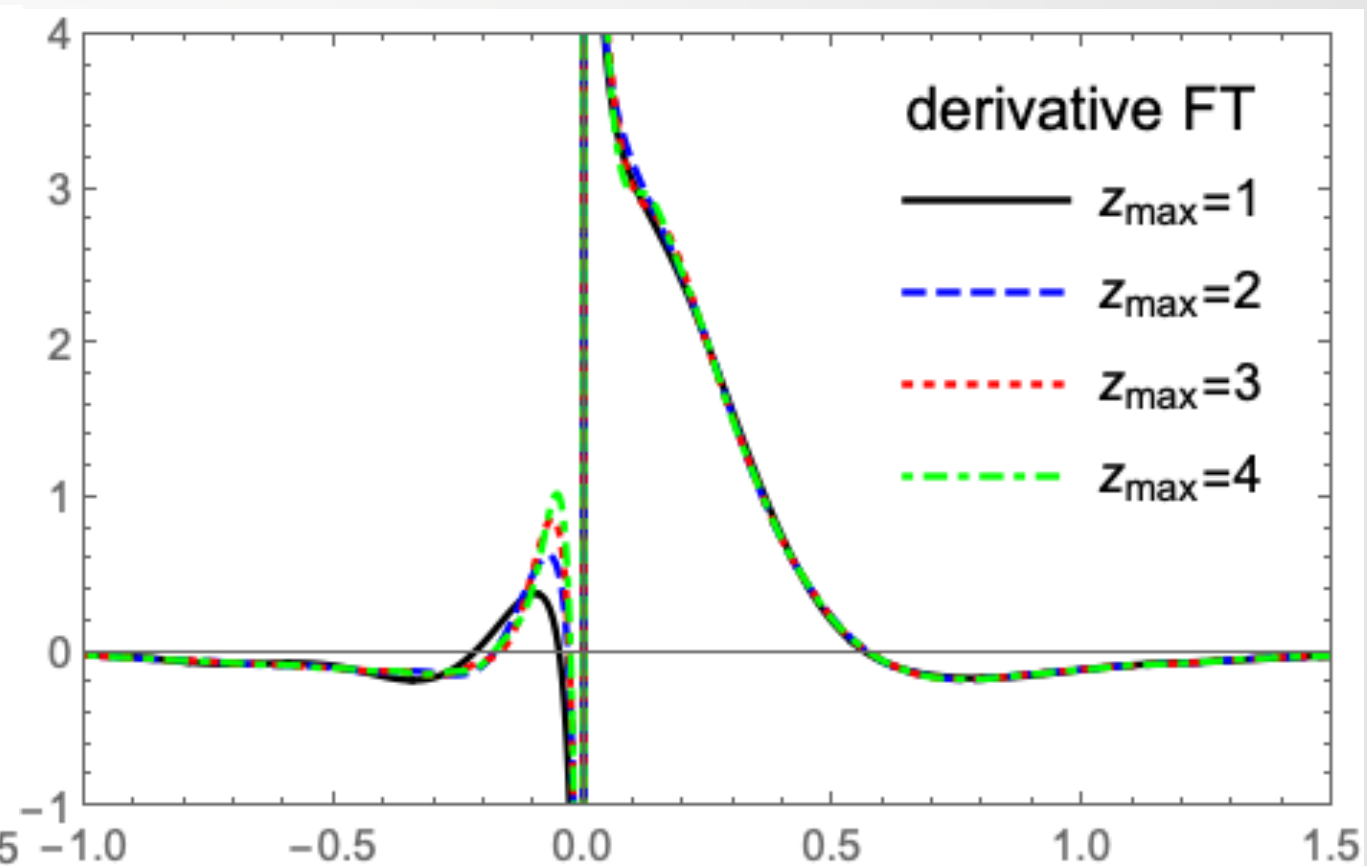
$$\tilde{q}(x) = \int_{-\infty}^{\infty} \frac{dz}{2\pi} e^{ixzP^z} \frac{ih'(z, P^z)}{x}$$

Sensitivity to z_{\max}

Ratio Scheme

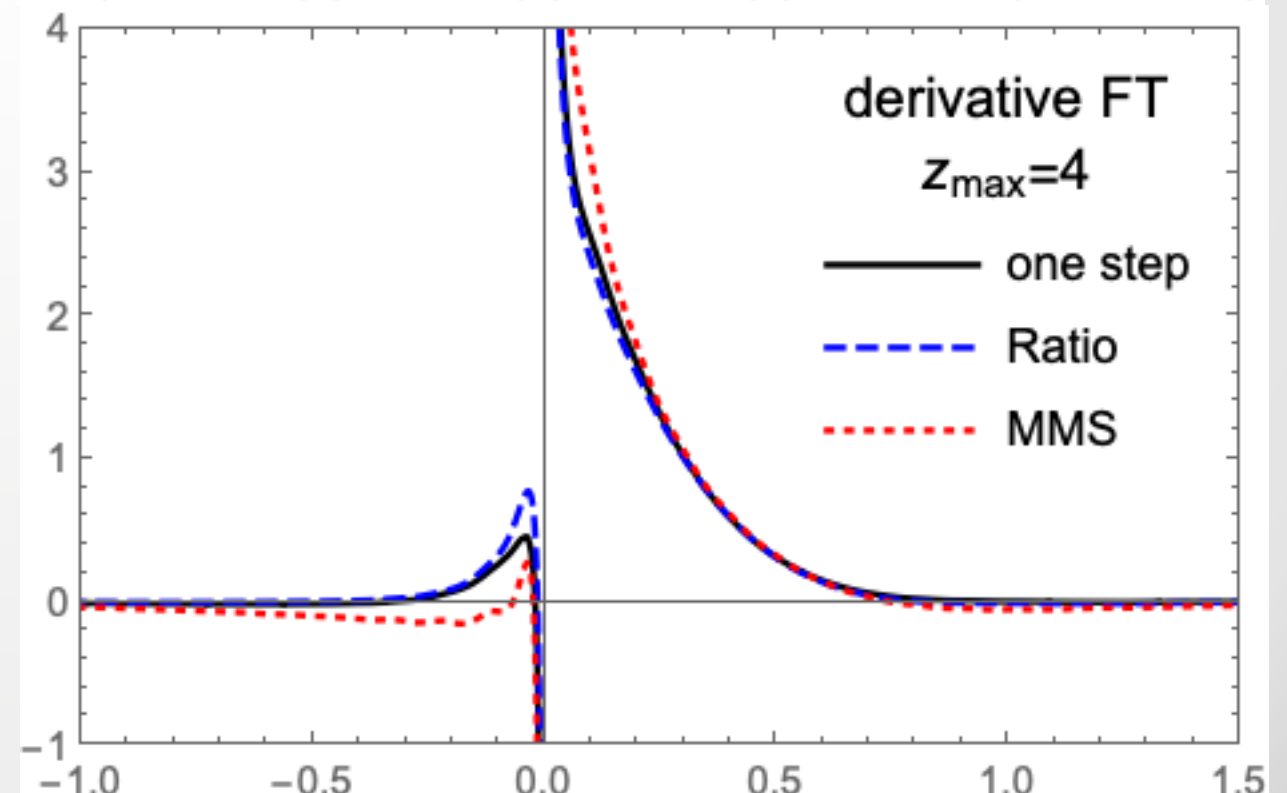
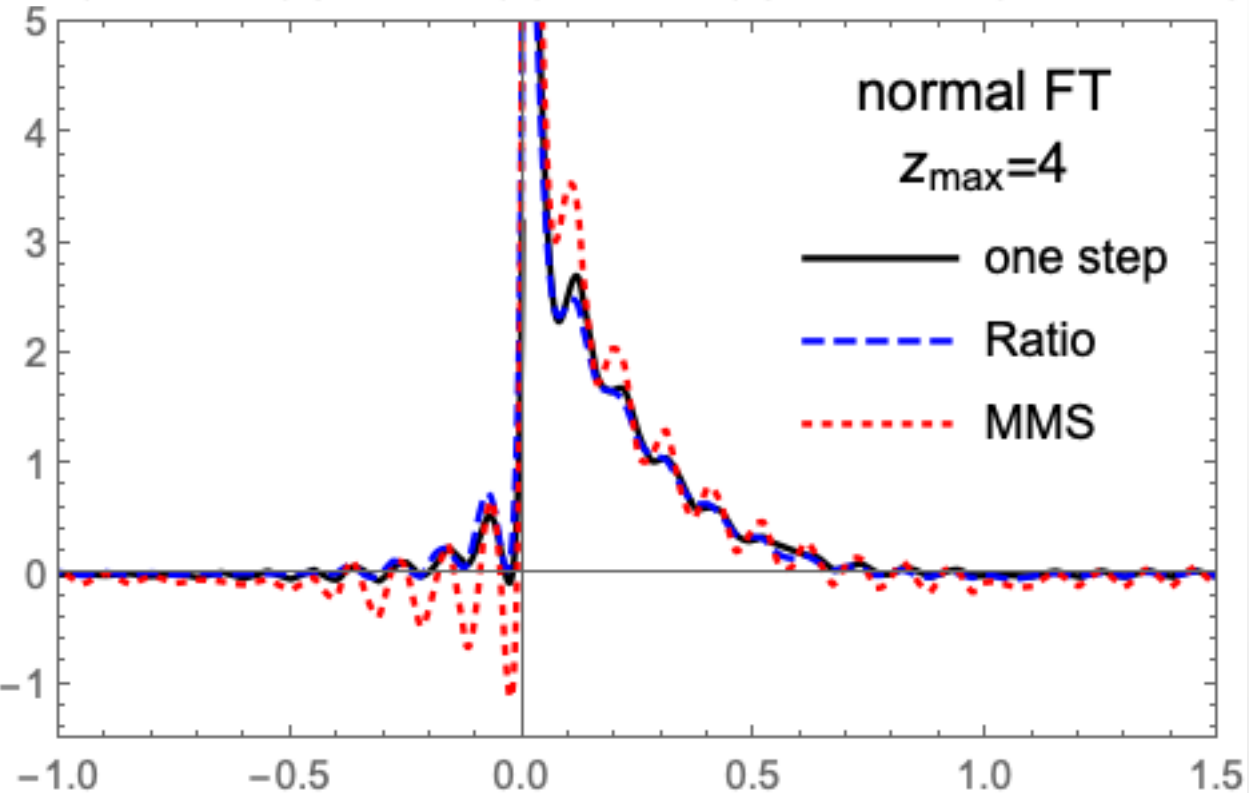
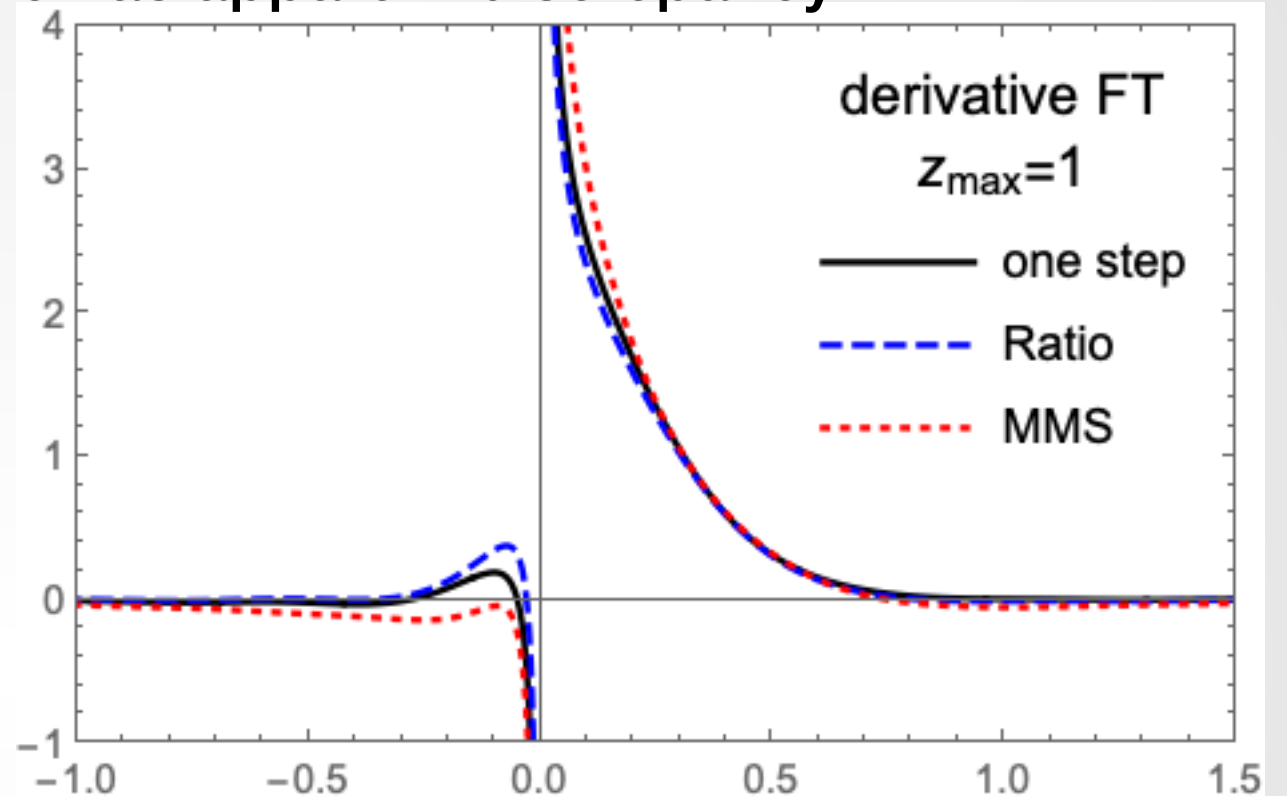
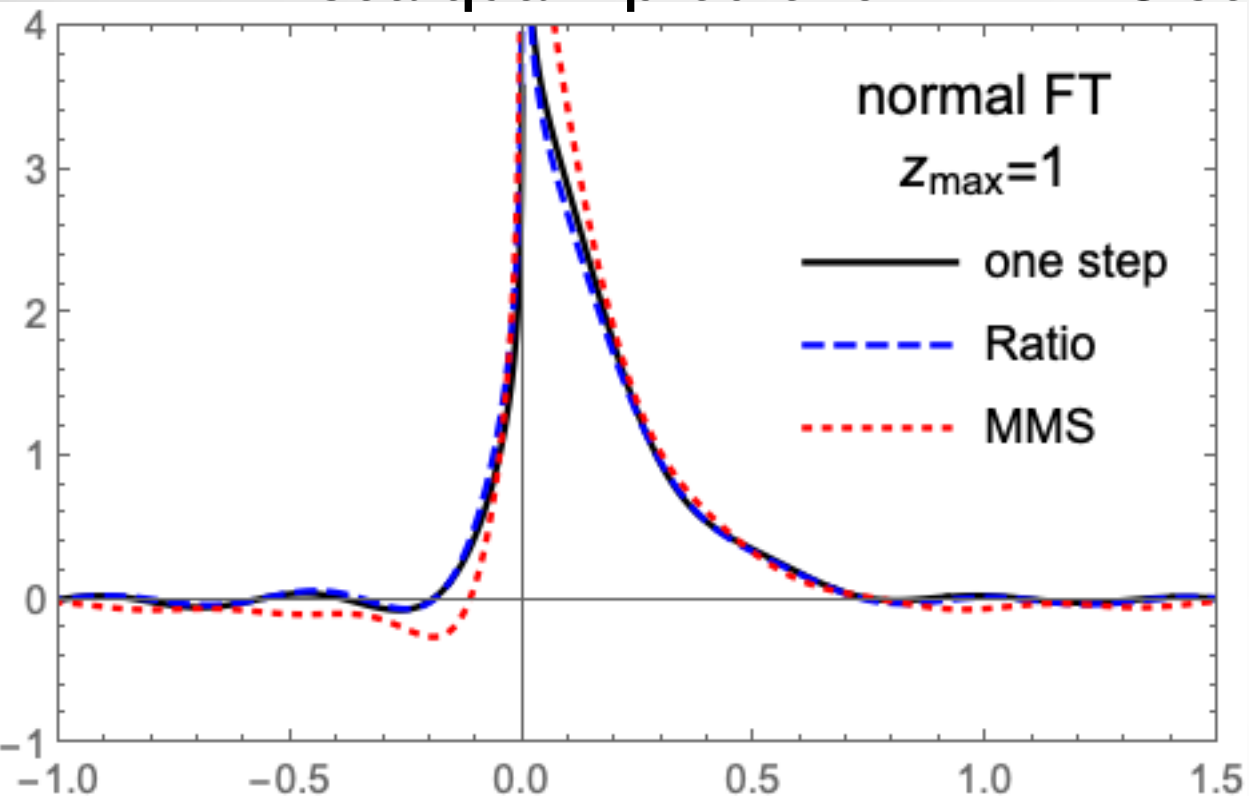


MMS Scheme



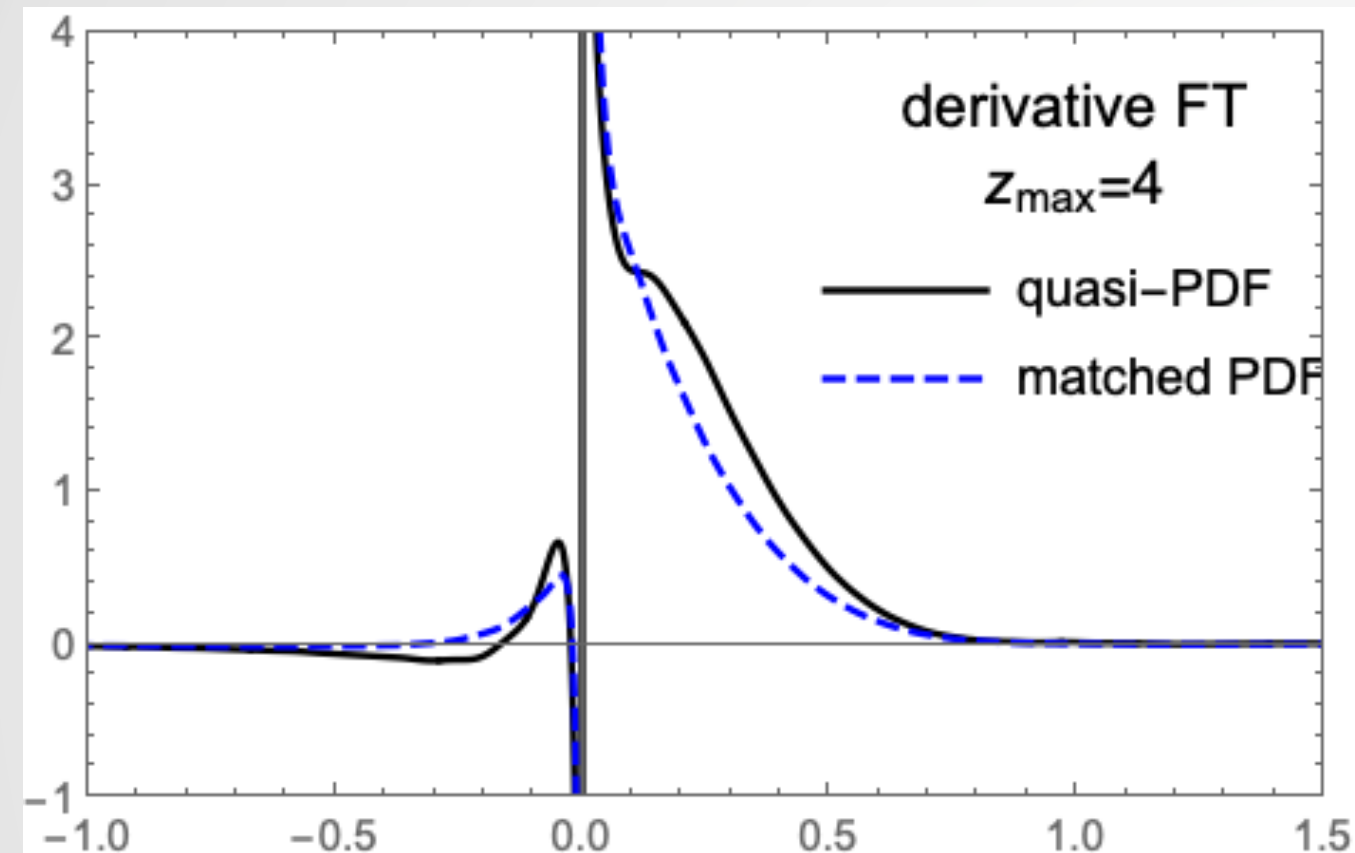
Final Result of the PDF

Ratio scheme shows more consistency with the one-step matching;
sea quark prediction in MMS scheme has apparent discrepancy.

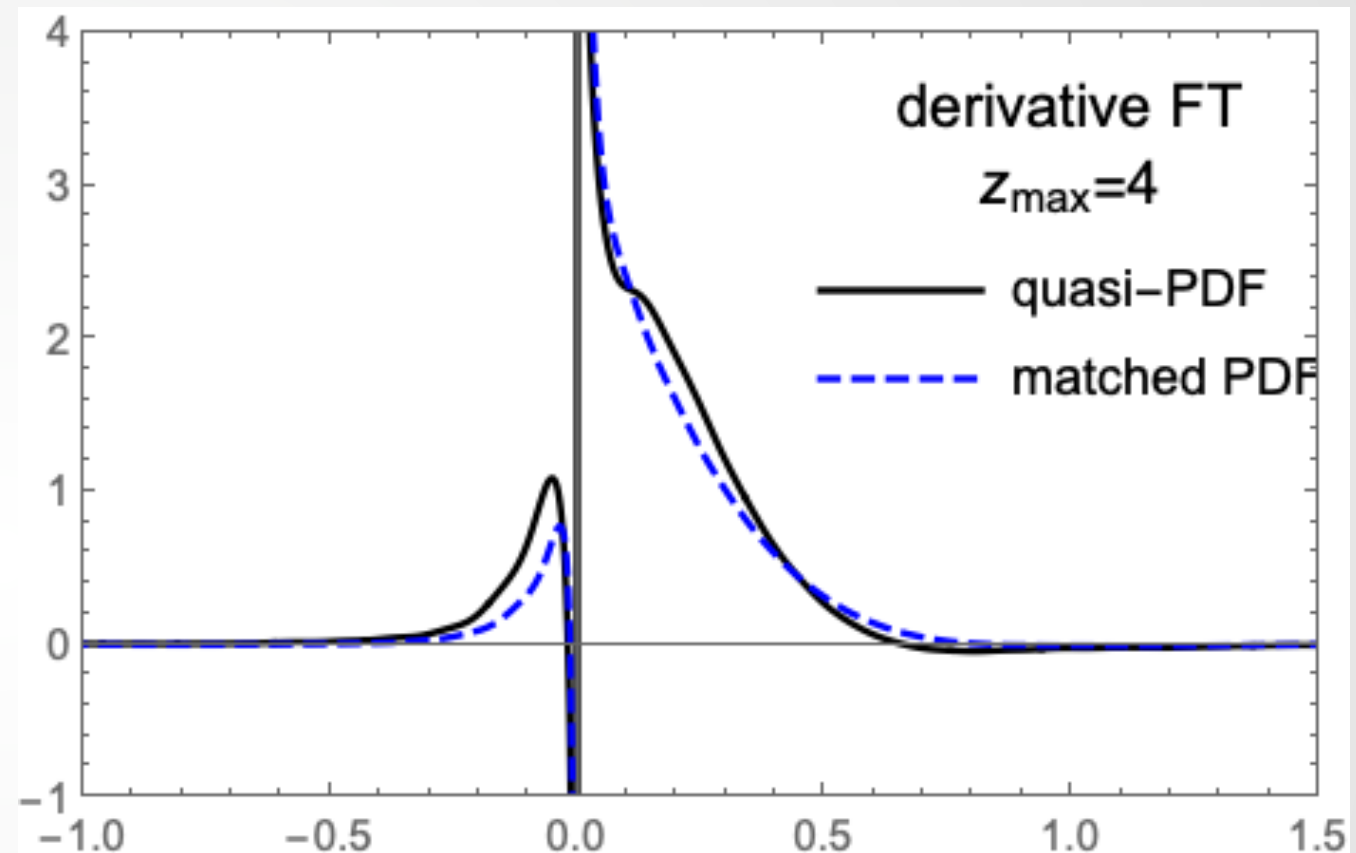


Effect of Matching

One-step matching



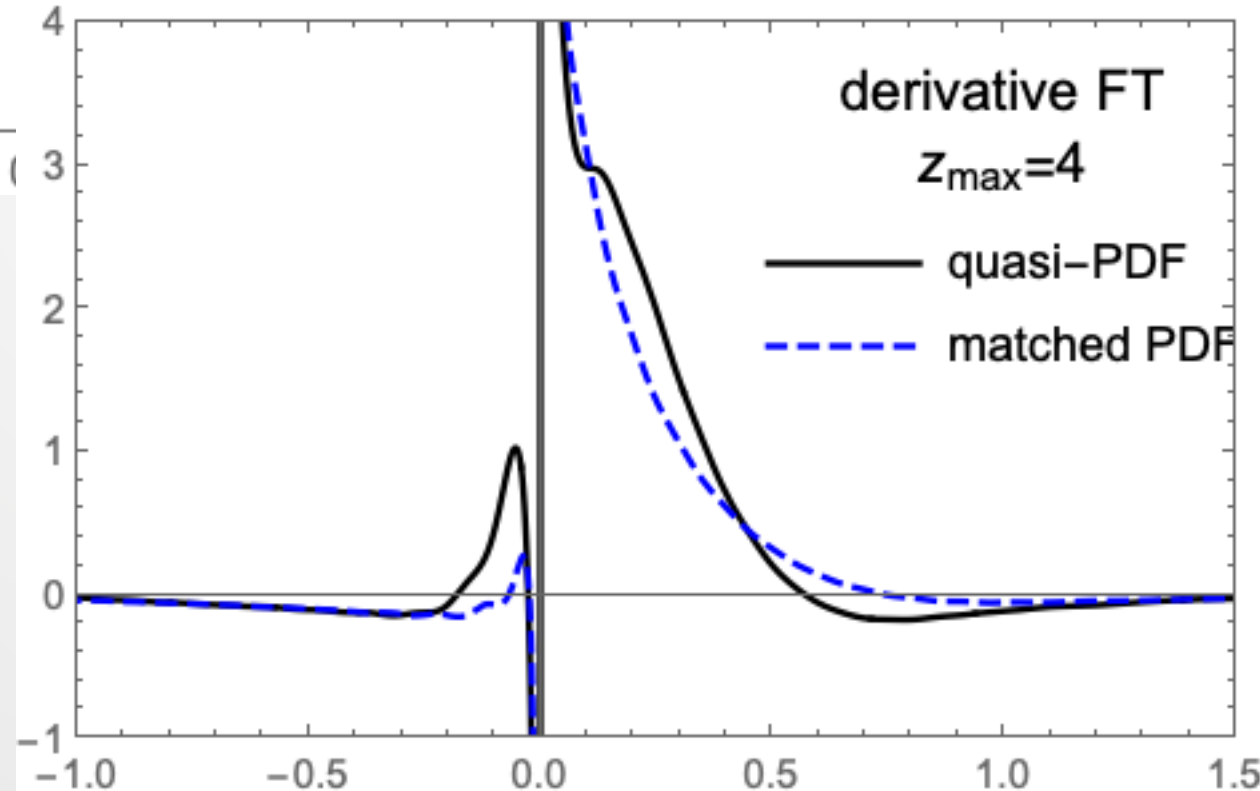
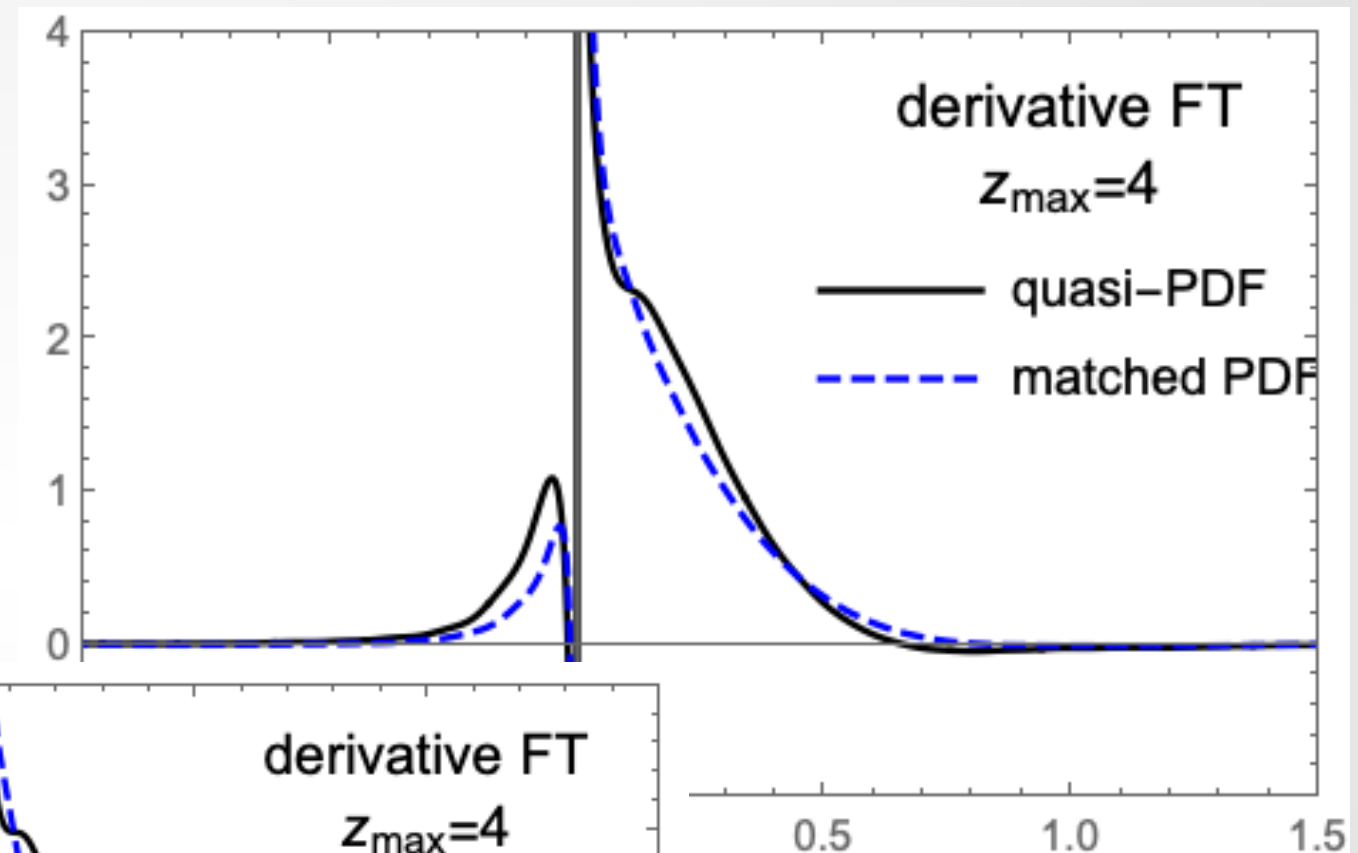
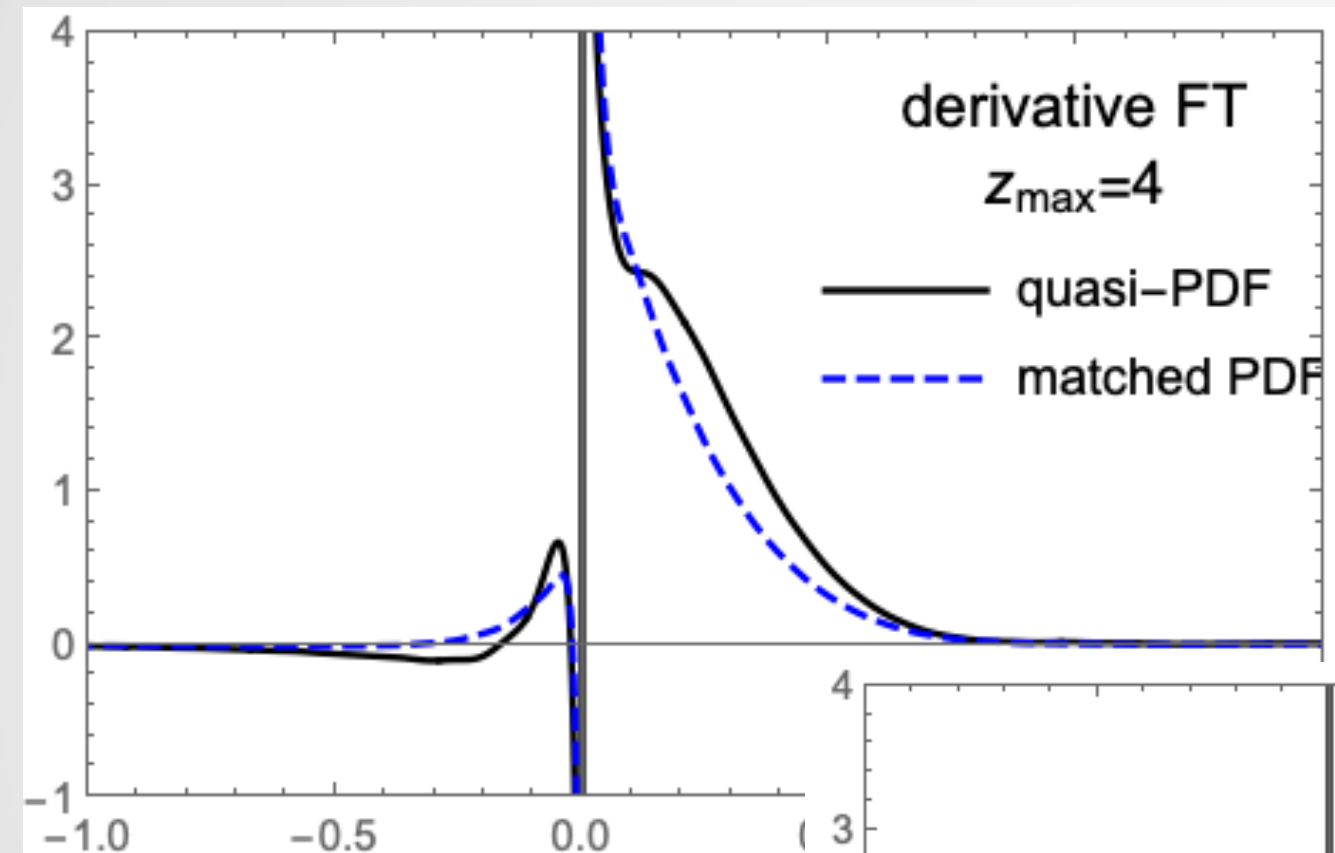
Ratio Scheme



Effect of Matching

One-step matching

Ratio Scheme



Conclusion

- The systematic procedure of lattice renormalization and perturbative matching for the quasi-PDF is already setup;
- Two-step matching is more effective in studying the renormalization scale dependence in coordinate space, while one-step matching is free from truncation errors in the Fourier transform of the conversion factor;
- The ratio scheme has a smaller conversion factor in coordinate space, which is favorable for perturbation theory and suffers less from the truncation effects in Fourier transform.

Outlook:

- Two-step matching is easier for higher-loop calculations. The scheme conversion factor can be calculated numerically, while the matching can be calculated with on-shell partons.